P1.6 LIGHTNING FORECASTING BEFORE THE FIRST STRIKE

James J. Stagliano, Bonnie Valant-Spaight, and J. Clayton Kerce

Propagation Research Associates, Inc.

1 INTRODUCTION

Bonaire, Georgia, September 11, 2008, 16:15 EST, a lightning strike sent 9 adults (coaches and principals) and one child to the hospital. A middle school football game was in progress. The game had just been called because a portable lightning detector sounded due to a strike about five miles from the field. The strike was the second from a rapidly developing storm cell (AP, 2008).

Cloud to ground (CG) lightning causes nearly a billion dollars of property damage and approximately 90 fatalities a year. Yet lightning warning facilities are minimal at best, and warnings primarily occur after the first strike even though there is a strong, but simple correlation with radar data and the vertical temperature profile. Such a simple correlation allows numerical weather prediction (NWP) models to forecast the lightning threat without the implementation of microphysics models to simulate cloud, hydrometeor development, and electrification.

A significant source of lightning concern is sporting activities that are played in open areas such as baseball, softball, football, soccer, and golf. In 1997, NOAA conducted a study of 3,239 lightning deaths over 35 years (Curran, 1997). They found that five times more people are killed by lightning in open fields or parks. Playgrounds and parks accounted for nearly 27% of lightning deaths, and golfers accounted for 5% of deaths during the period. Table 1 below shows the results of the NOAA study.

Table 1. Lightning fatality statistics 1959-1994 (Curran, 1997)

Activity	Deaths	Percent
Open field, park, playground, etc.	868	26.8%
Under trees	444	13.7%
Water related, fishing, boating, swimming, etc.	262	8.1%
Golf course, including sheltering under trees	159	4.9%
Driving tractors, farm equipment, heavy road equipment, etc.	97	3%
Telephone related	78	2.4%
Radios, transmitters, aerials	23	0.7%
Other/Unknown	1,308	40.4%

Corresponding Author: James J. Stagliano, Propagation Research Associates, 1275 Kennestone Circle, Suite 100, Marietta, GA 30066 jim.stagliano@pra-corp.com

On the other hand if you assume that 50% of the U.S. population visits open fields, parks, or playgrounds at least once each year and that half of them can be found at least occasionally under trees, the statistics indicate the likelihood is one lightning death per 5.3 million visiting open fields, parks, or playgrounds, and one in 5.2 million of those wandering under trees. Furthermore, these statistics do not account for injuries that occur due to lightning every year which will be far greater in number than deaths.

Clearly an early warning system would reduce death and injury due to lightning. This paper briefly describes a simple cloud electrification model forming the basis for nowcasting and forecasting products for determining the lightning threat. The products are applied to different events including the one that occurred in Bonaire, Georgia.

2 ELECTRIFICATION MODEL

The electrification model refers to process by which charge is separated within the cloud, creating the significant electric field and subsequent electrical discharge we call lightning. Though this simple model explained herein cannot explain the complex charge structure within a cloud, it captures the essence of algorithm to nowcast and forecast CG lightning.

The model begins with moist air rising into the atmosphere. As it rises, it expands and cools, condensing into water droplets. As the water droplets rise above the -10^{o}C level, ice crystals begin to form. The ice crystals grow into graupel through the riming process. As graupel is formed, the radar signature begins to be become significant. The graupel descends, colliding with ice crystals at lower altitudes. The collisions result in charge transfer between the graupel and the ice crystals. The ice crystals and graupel are subsequently advected to higher altitudes through updrafts, with the ice crystals reaching a higher altitude. The result is charge separation and an associated electric field. As the electric field increases, the temperature at which ice can form increases, providing a positive feedback mechanism for the charge separation and electric field generation.

The important aspects of this process are the development of the radar signature and the increasing charge separation. The latter results in an increasing electric field which can be measured at the ground with an E-field mill device. The radar reflectivity becomes significant as sufficient ice crystals and graupel form. The altitude of the -10^{o}C level identifies the altitude where ice formation begins. The maximum altitude at which the reflectivity is detected identifies the height at which the ice transporting the charge is attaining. Therefore, the height of the reflectivity above the threshold is a proxy for the electric field development and the subsequent lightning discharge.

3 LIGHTNING PREDICTION SYSTEMS

Current lightning prediction systems fall into two categories, those requiring strikes to provide warning and those that can predict before the first strike. They also come in a variety of sizes from national networks to hand held detectors and utilize different techniques and technology.

3.1 Post Strike Prediction Systems

Post strike prediction systems rely on a single or multiple strikes to provide warning of lightning threat. These units fall into two categories, small hand held units that register strikes within a certain range, and systems that utilize data from a lightning detection network.

The former come in a variety of sizes from small handheld units to antennas that connect to a PCI card within a computer. Both of these units detect the electromagnetic pulse produced by the discharge. The hand held units estimate the distance from the sensor to the discharge and gives visual and audible warnings of lightning strikes in the area.

The computer based sensor operates similarly. However, it utilizes a directional antenna and associated signal processing to determine the location, range and azimuth of the discharge. The result is displayed on a georeferenced display on the computer screen.

The second type of post strike prediction system utilizes a network of lightning detection sensors to determine the location and characteristics of the discharge. A number of discharge events are needed to estimate the advection of the lightning. From the time series, nowcasts of lightning threat are produced.

Obviously lightning warning using the post discharge devices are insufficient to warn before the first strike. In the Bonaire event, the responsible parties had a hand held device but it did not give sufficient warning to prevent the tragedy.

3.2 Pre-Strike Prediction

Prestrike lightning prediction utilizes data which are precursors to lightning generation. The precursors include the electric field at the ground and characteristics of certain radar products.

The electric field is a measure of the electrical potential energy due to the difference in charge between two surfaces (cloud and ground). When the electric field attains a critical value, the breakdown potential, discharge can occur. The electric field is measured with an electric field mill sensor which in its basic form alternately exposes and shields electrodes from the background electric field. This results in a current produced between the electrodes that is proportional to the electric field strength.

The primary issue with these kinds of meters is threat the breakdown voltage varies with atmospheric conditions and thus with different climatic regimes and/or times of the year. Thus warning threshold that apply say in Florida are not applicable to elsewhere. This of course is not a problem provided tuning is performed for a particular installation. The tuning requirements will require significant amounts of event data.

As with the handheld and the smaller computer based post strike sensors, electric field monitors can be relatively portable and be collocated with audible warning systems.

A second pre-strike prediction technique uses radar products as a proxy for the lightning threat potential. A number of manufacturers use different products such as vertically integrated liquid and echo tops products to derive some estimate of the likelihood of lightning. These techniques of course rely on the availability of radar data. The advantage of this technique is the ability to begin forecasting as the cells develop. In the next section a simple radar product technique is explored.

4 LIGHTNING NOWCASTING VIA RADAR

A number of studies have indicated a correlation between cloud to ground (CG) lightning and relatively high radar reflectivity values attained at significant altitude. Vincent (2003) and later Wolf (2007) described a relatively simple correlation between CG lightning strikes 10-20 minutes after volume collection and the altitude associated with the 40 dBZ reflectivity level with respect to the height of the -10℃ level of the collected data volume. Wolf (2007) extended the correlation to include “frequent” (greater than 10 strikes in a 5-minute period) and “numerous” (greater than 20 strikes in a 5-minute period) CG activity. Figure 1 shows the probability for the different states, no CG lightning, CG lightning, frequent CG lightning, and numerous CG lightning (Wolf, 2007) with respect to the relative height of the 40-dBZ radar reflectivity to the -10℃ altitude. For the algorithm, the probability density functions described in Figure 1 are transformed into piece-wise third-degree polynomials through the fitting of the data with cubic splines. There is one set of functions for each characteristic data set (CG, Frequent CG, and Numerous CG).

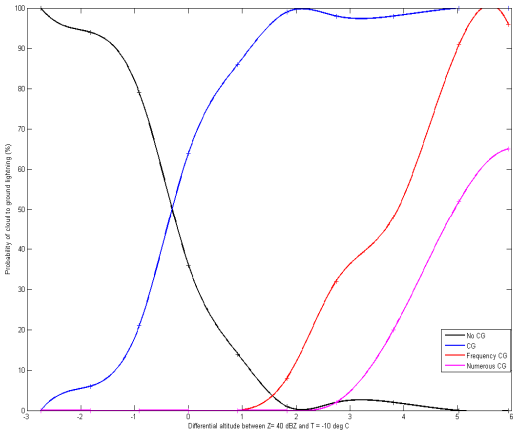

Figure 1. CG lightning probability as a function of the height of the 40 dBZ echo relative to the -10℃ level .

4.1 Lightning Nowcast Model

A representative algorithm to generate the lightning probability would have as input the radar reflectivity threshold (nominally 40 dBZ) (Z_{th}), the height of the -10℃ level (h_{-10}), and the radar data volume. The algorithm begins by reading the radar data volume (Level II data) into memory. Each sweep or elevation slice is examined for radar reflectivity values greater than the threshold. Assuming a standard

refractive atmosphere (4/3 R_E approximation), the height of a particular sample is given by (Rinehart, 1991),

$$H = \sqrt{r^2 + R'^2 + 2rR'\sin(\phi_{el})} - R' + H_0 , \quad (1)$$

where r is the range from the radar, R' is the Earth's effective radius, $4/3R_E$, φ_{el} is the elevation angle, and H_0 is the antenna height above the ground. This height is projected onto the Earth's surface via a simple cosine relation,

$$R_{flat} = r\cos\phi_{el} . \quad (2)$$

Once the entire volume has been traversed, the resultant geo-referenced product denoted by **H** gives the heights of radar reflectivity echoes greater than the threshold. Subtracting the height of the -10℃ level (h_{-10}) from **H** gives a new product of relative heights, relative to the -10℃ level,

$$\mathbf{H}_{litn} = \mathbf{H} - h_{-10} . \quad (3)$$

The lightning probability is subsequently determined by applying the piece-wise polynomials to the product $\mathbf{H}_{litn}$. The result is three polar products representing CG, Frequent CG, and Numerous CG, respectively. These can be applied as raster layers to a mapping system or converted into vector quantities (shape files) for direct application in a mapping application.

The algorithm was applied to the events of Ft. Worth, TX on April 6, 2003. Figure 2 shows the base reflectivity PPI. Figure 3 through Figure 5 shows corresponding PPI's for the CG lightning threat probability, Numerous CG lightning threat probability and Frequent CG lightning threat probability.

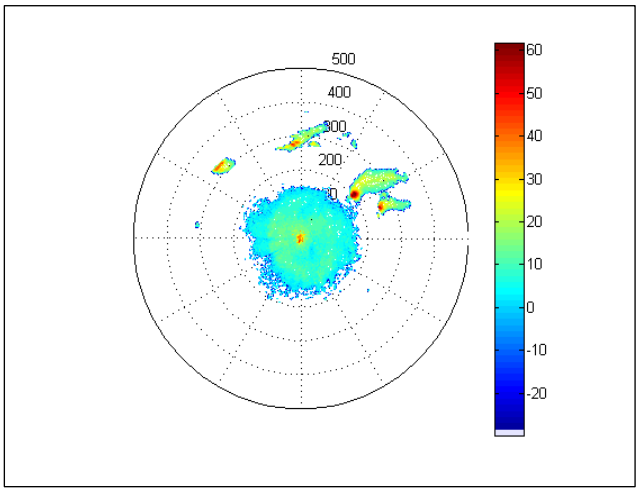

Figure 2 PPI reflectivity display of the Ft. Worth area, April 6, 2003 at 0809 GMT.

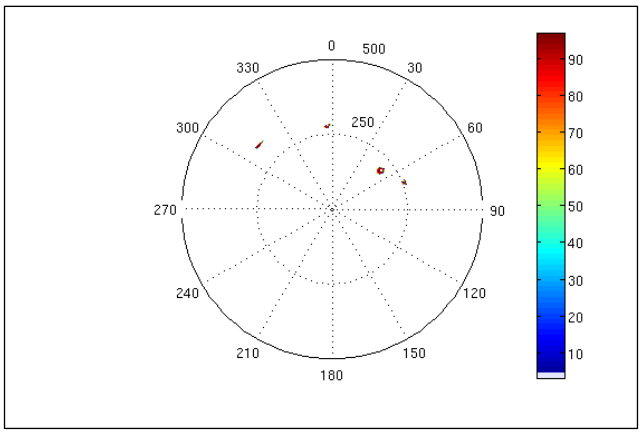

Figure 3 PPI showing the cloud to ground lightning probability.

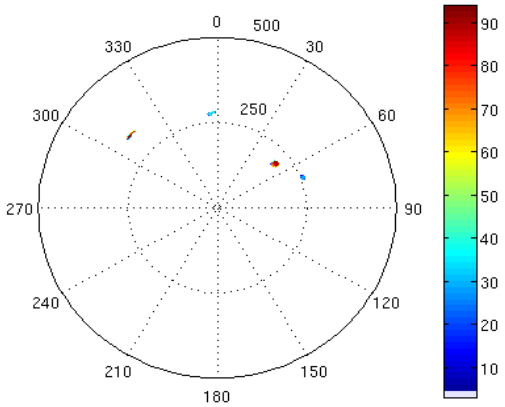

Figure 4 PPI showing the probability of frequent cloud to ground lightning

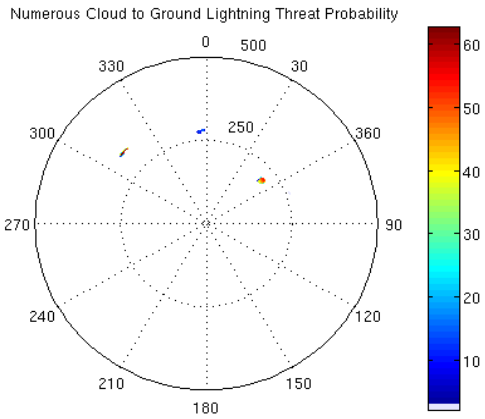

Figure 5 PPI display showing the numerous CG lightning threat probability.

However, it is likely these cells are in motion as well which would be defined by the storm track file. Using the properties of the cell defined in the storm track product, the lightning threat can be forecast along the path.

The incident in Bonaire, GA on September 11, 2008 was also evaluated. The lightning discharge that struck the football field occurred at 1815 EST. The cell that produced the lightning developed near the field. Figure 6 through Figure 13 shows the base reflectivity and the associated lightning probabilities at 1800, fifteen minutes before the field was struck. At this time, 1800, the cell is showing 98% probability of CG lightning and 60% probability of frequent CG lightning within the next 10-20 minutes.

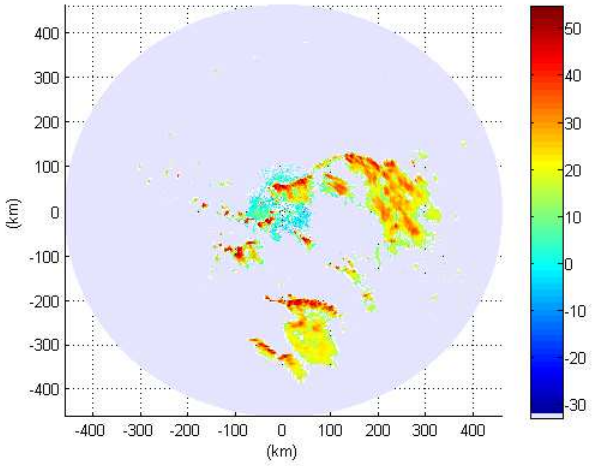

Figure 6 Base reflectivity product of KJGX September 11, 2008 at 1800 EST. The cell to the southwest of the radar site (center of image) produced the lightning discharge that struck the football field.

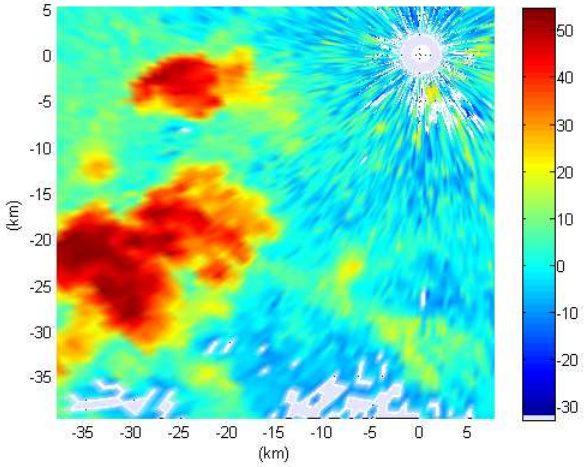

Figure 7 Base reflectivity product zoomed in to the area surrounding the football field.

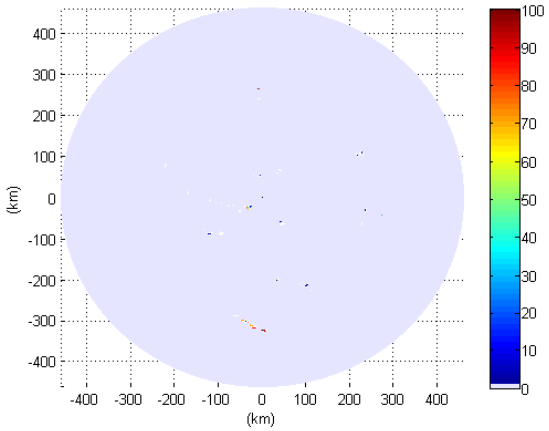

Figure 8 The probability of CG lightning based upon the algorithm. The cell that generated the strike on the football field had a probability of 98% of producing CG lightning discharges.

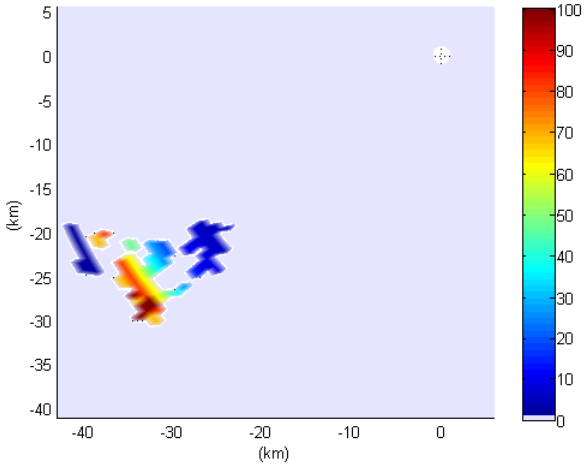

Figure 9 The probability of CG lightning zoomed in to the area around the football field.

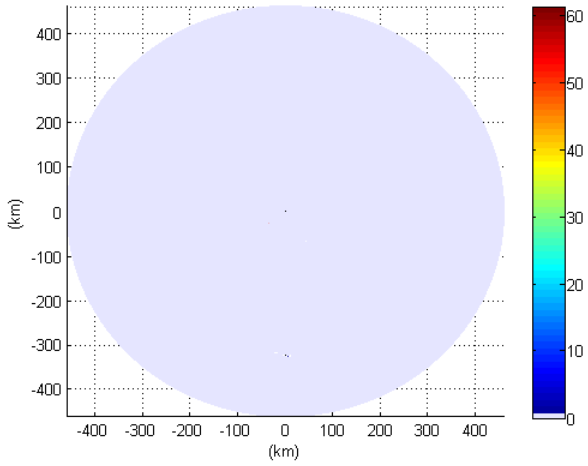

Figure 10 The probability of Frequent CG lightning (> 2 str/min) based upon the algorithm. The cell that generated the strike on the football field had a probability of 60% of producing Frequent CG lightning discharges.

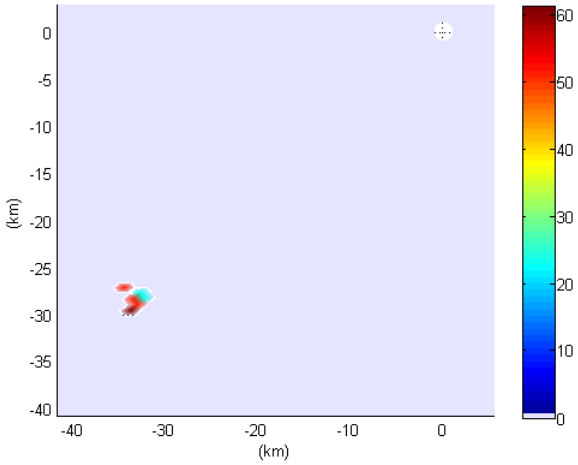

Figure 11 The probability of Frequent CG lightning zoomed in to the area around the football field.

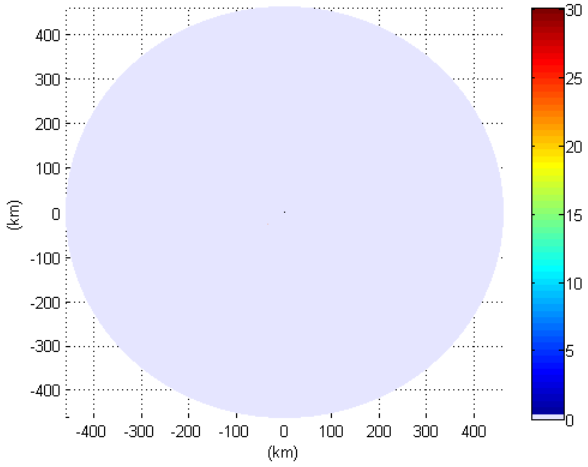

Figure 12 The probability of Numerous CG lightning (> 4 str/min) based upon the algorithm. The cell that generated the strike on the football field had a probability of 20% of producing Numerous CG lightning discharges.

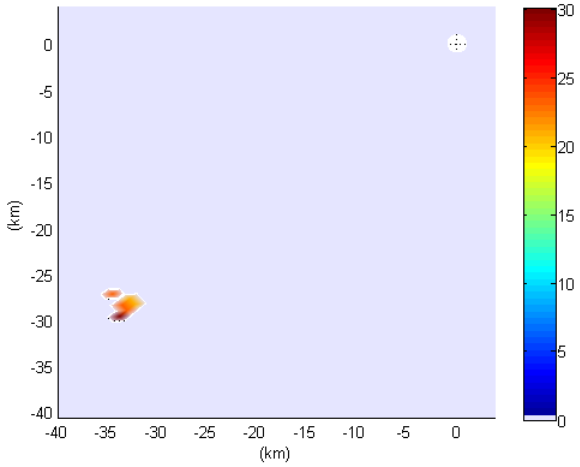

Figure 13 The probability of Numerous CG lightning zoomed in to the area around the football field.

5 Lightning Forecasting with NWP

WRF is the current numerical weather prediction (NWP) software used by the National Weather Service as well as other government agencies. As WRF does not contain an electrification module, previous work using WRF to forecast lightning has looked primarily on the cloud microphysics (McCaul 2007). Even this is somewhat limited in that the microphysics model provides for six hydrometeor species and only a single precipitating ice species. McCaul (2007) selected graupel as the ice species as they were concerned with forecasting lightning and as described in the electrification section, graupel is a critical component in the charge separation process.

The approach taken at PRA to utilize WRF to produce six hour forecasts of CG lightning was significantly different. PRA

used a vanilla WRF model and simply used the reflectivity fields and the vertical temperature profile fields as the proxies for CG lightning. Using these fields, the PDF's discussed previously were applied to the WRF output data to generate the lightning threat probabilities.

The WRF lightning forecast process was applied to the tornado event in Enterprise, Alabama of March 1, 2007. In this event, an EF4 tornado tore through the downtown area, destroying an elementary school and the adjoining high school. Of course for our purposes, we are not concerned with the tornadic event but rather the lightning.

The WRF domain was established with the nearest WSR-88D (KEOX) as the center and there are 45 grid points on either side of the center. With 3 km grid spacing, this models a 135 km radar range. This configuration of the WRF domain facilitates comparison with radar results.

Figure 14 shows the ground level reflectivity field extracted from WRF. It is interesting to note the strongest returns are actually north and northwest of the radar (Enterprise is about 20 km to the southwest). Using the algorithm described above, the probability of CG lightning is nearly 100% throughout most of the coverage area as shown in Figure 15. However, the probability of frequent CG lightning is reduced through most of the region except in the areas with the strongest returns and here the probability of numerous CG strikes is reduced to 60 – 70% as shown in Figure 16 and Figure 17 respectively.

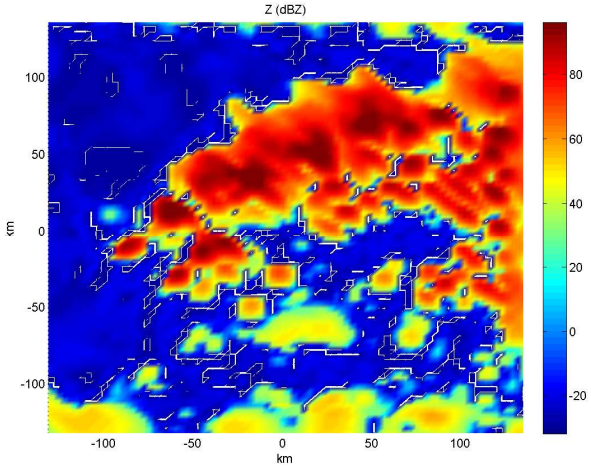

Figure 14 Ground reflectivity field generated by WRF for KEOX region March 1, 2007 at 1340 UTC.

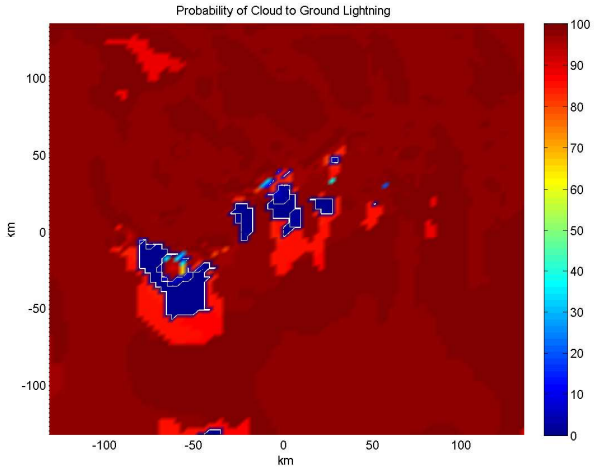

Figure 15 CG lightning threat probability for the KEOX region March 1, 2007 at 1340 UTC

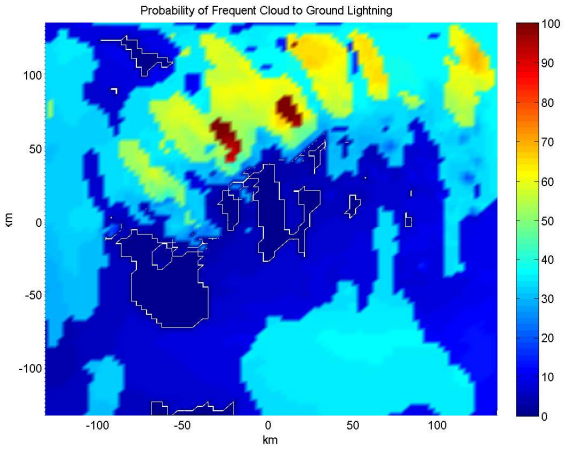

Figure 16 Frequent CG lightning threat probability for the KEOX region March 1, 2007 at 1340 UTC

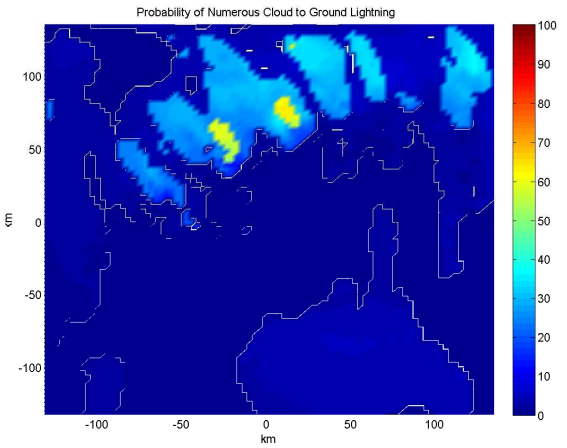

Figure 17 Numerous CG lightning threat probability for the KEOX region March 1, 2007 at 1340 UTC

A six hour WRF forecast was produced for the Bonaire event. The WRF forecast produced at the 3 km grid space resolution failed to defined the convective cells and hence forecast the lightning. Figure 18 shows the base reflectivity product produced with the 3 km grid spacing and Figure 19 is the corresponding CG lightning threat product. At the 3 km grid spacing, the WRF forecast failed to capture cell development and the associated lightning threat.

Reducing the mesh size by a factor of 3 to 1 km between grid points, the development of convective cells was observed, as shown in Figure 20. . The WRF forecast at this grid spacing captured the development of the pertinent cell (lower left hand corner) and its associated lightning threat as shown in Figure 21 to Figure 23.

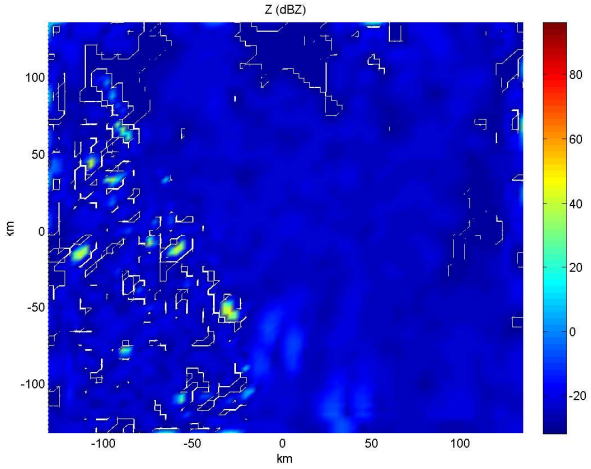

Figure 18 WRF base reflectivity field with 3 km grid spacing. With this spacing, WRF failed to capture the convective development that led to the CG lightning.

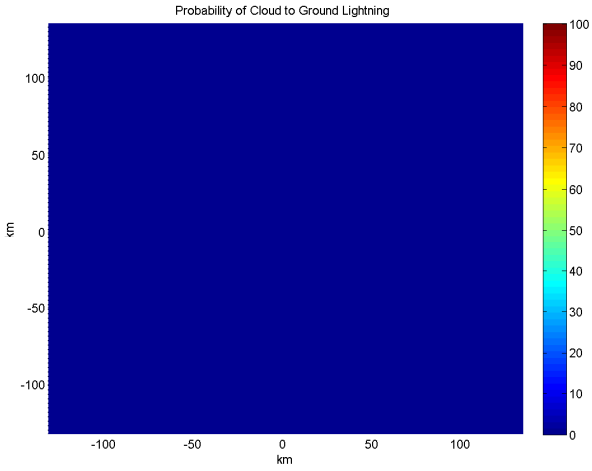

Figure 19 CG lightning threat probability forecast based on the WRF forecast produced with 1 km spacing.

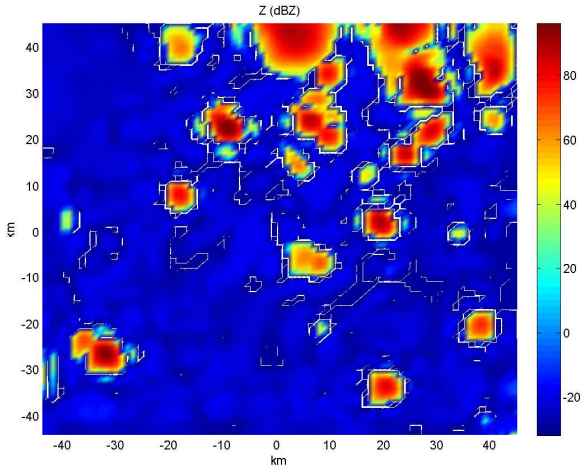

Figure 20 WRF base reflectivity field with a 1 km grid spacing. With this spacing, WRF captured convective development that led to the CG lightning in the region, however the cell locations were not correct.

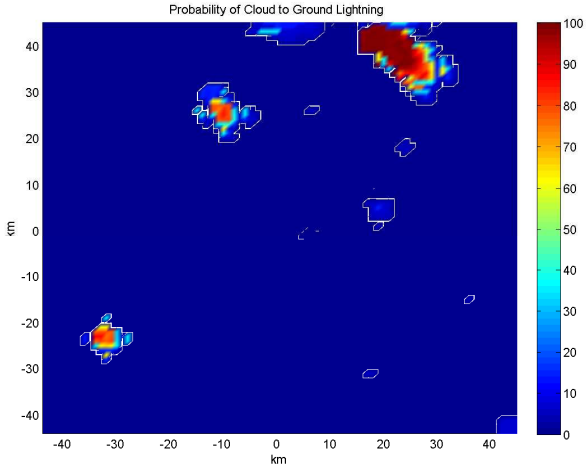

Figure 21 CG lightning threat probability forecast based on the WRF forecast produced with 1 km spacing.

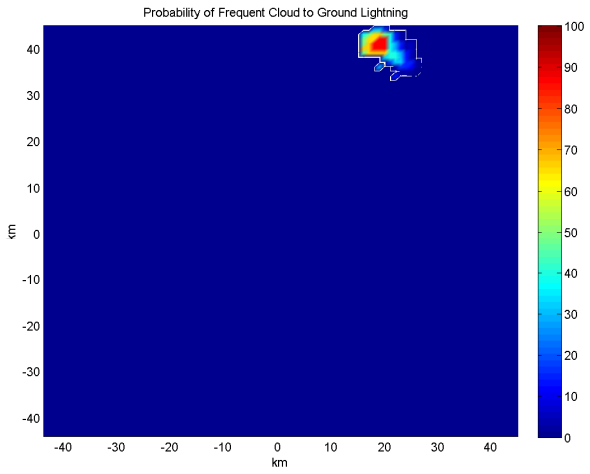

Figure 22 Frequent CG lightning (> 2 str/min) threat probability forecast based on the WRF forecast produced with 1 km spacing.

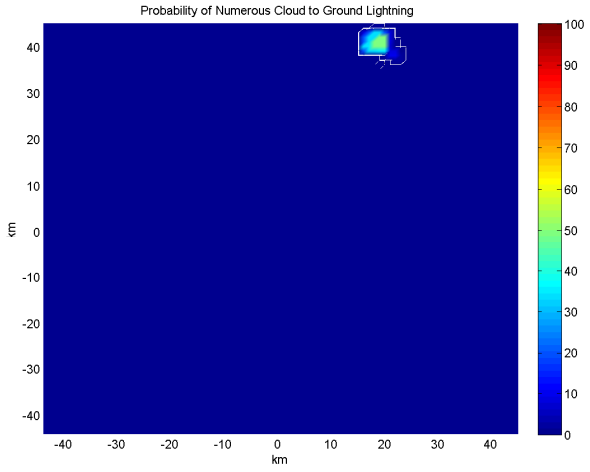

Figure 23 Numerous CG lightning (> 4 str/min) threat probability forecast based on the WRF forecast produced with 1 km spacing.

With the data available for the initial conditions, WRF would not have been able to forecast the lightning strike with the 3 km grid spacing, however at the 1 km grid spacing it would predict lightning threat development in the area.

6 CONCLUSION

A simple algorithm was described for nowcasting lightning threat based upon the maximum height attained by radar reflectivities above 40 dBZ and the height of the –10 oC level. The algorithm was applied to an event that occurred September 11, 2008 in Bonaire, Ga and it was determined that a warning based on the algorithm output would have provided enough time to clear the football field before it was struck.

WRF generates fields including the temperature profile and estimates of the reflectivity. WRF six hour forecasts were generated for Enterprise, AL on March 1, 2007 at 1300. The forecast predicted high probability of CG lightning throughout the region. However, when a WRF forecast was conducted for the Bonaire, GA event, WRF failed to produce the cells that generated the lightning with 3 km grid spacing but did predict some cells at different locations in the forecast area at the 1 km grid spacing. Thus, WRF provided facility in predicting lightning with respect to significant severe weather events, but only captured initiation of isolated lightning producing cells in a region at fine grid resolution.

7 ACKNOWLEDGEMENTS

This work was funded by the National Weather Service under contract WC133R-08-CN-0142**.**

8 REFERENCES

Associated Press, 2008: Lightning strike causes injuries at football game, *http://www.wtvm.com/Global/story.asp?S=8996051.*

Bringi, V.N. and V. Chandrasekar, 2001: **Polarimetric Doppler Weather Radar**, Cambridge University Press, pp. 636.

Brown, B., R. Bullock, J.H. Gotway, C. Davis, D. Ahijevych, E. Gilleland, L. Holland, 2007: New tools for evaluation of numerical weather prediction models using operationally relevant approaches, *Battlespace Atmospheric and Cloud Impacts on Military Operations, 6-8 November, Chestnut Hill, Massachusetts*.

Conway, J.W. and M. Eilts, 2005: The Lightning Decision Support System:Predicting lightning threat utilizing integrated data sources, *Conference on Meteorological Applications of Lightning Data 8-14 January, San Diego, California.*

Dixon, M and G. Wiener, 1993: TITAN: Thunderstorm Identification, Tracking And Nowcasting, *J. Atmos. Tech*, **10**, 785-797.

Ebert, B., 2005: Verification of Forecasts, *WWRP Nowcasting Training Workshop, 28 November-9 December, Pretoria, Republic of South Africa*.

Gelb, A., 1974: **Applied Optimal Estimation**, MIT Press, pp. 374.

Georgia High School Association (GHSA), 2006: Lightning Detector Requirements, http://www.ghsa.net/?q=node/1.

Gin, R.A.A. and C.A.A. Beneti, 2004: Cloud-to-ground lightning flash density in the south and southeastern of Brazil: 1999-2003, *Fourth EMS Annual Meeting 26 – 30 September, Nice, France.*

Hodanish, S., 2006: Colorado Lightning Resource Page, *http://www.crh.noaa.gov/pub/ltg.php.*

Hogan, R.J., A.J. Illingworth, and E.P. Krider, 2002: Polarimetric Radar Observations of storm Electrification and Lightning, *Second European Conference on Radar Meteorology, 18-22 November, Delft Netherlands*.

Johnson, J.T., P.L. MacKeen, A. Witt, E.D. Mitchell, G.J. Stumpf, M.D. Eilts, K.W. Thomas, 1998: The Storm Cell Identification and Tracking Algorithm: An Enhanced WSR-88D Algorithm, *Weather and Forecasting*, **13**, 263-276.

Lund, N.R., D.R. MacGorman, W.D. Rust, T.J. Schuur, P.R. Krehbiel, W. Rison, T. Hamlin, J.M. Straka, and M.I. Biggerstaff, 2008: Relationship between lightning location and polarimetric radar signatures in an MCS, *Third Conference on Meteorological Applications of Lightning Data 21-24 January, New Orleans, Louisiana.*

McFarquhar, G.M., M.S. Timlin, R.M. Rauber, B.F. Jewett, J.A. Grim, A.M. Smith, and D.P. Jorgensen, 2005: Observations of the Horizontal and Vertical Variability of Cloud Hydrometeors in Stratiform Regions behind Bow Echoes: Implications for Mesoscale Models, *11th Conference on Mesoscale Processes, 22-28 October, Albuquerque, NM*.

Nelson, S., V. Adams, D. Selove, 1998: Lightning-Associated Deaths -- United States, 1980-1995, *MMWR*, **47**, 391-394.

Orville, R.E. and G.R. Huffines, 2001: Cloud to ground lightning in the United States: NLDN results in the first decade, 1989-1998, *Mon. Wea. Rev.*, **129**, 1760-1776.

Passarelli, R., 2005: Personal Communication – Discussion as to how graduate students would take a Tesla coil into refrigerator, blow on it and observe the creation of ice crystals, *32nd Conference on Radar Meteorology, 22-28 October, Albuquerque, NM*.

Rinehart, R.E., 1991: **Radar for Meteorologists Second Edition**, Knight Printing Company, Fargo, North Dakota, 334.

Vincent, B.R, L.D. Carey, D. Schneider, K. Keeter, and R. Gonski, 2003: Using WSR-88D reflectivity data for the prediction of cloud-to-ground lightning: A North Carolina study. *Nat. Wea. Digest*, **27**, 35-44.

Wolf, P., 2007: Anticipating the Initiation, Cessation, and Frequency of Cloud-to-Ground Lightning, Utilizing WSR-88D Reflectivity Data, National Weather Association, *http://www.nwas.org/ej/2007/2007.php.*

Wang, Z.,2007: ttp://www.weather.gov/code88d/code_b10.html

Zajac, B.A. and S.A. Rutledge, 2001: Cloud to ground lightning activity in the contiguous United States from 1995 to 1999, *Mon. Wea. Rev.*, **129**, 999-1019.

Zrnić, D.S., 2007: Polarimetric upgrade of the WSR-88D (NEXRAD) network, *33rd Conference on Radar Meteorology 6–10 August 2007, Cairns, Queensland.*